Identification of Individual Nucleotides in the Bacterial Ribonuclease P Ribozyme Adjacent to the Pre-tRNA Cleavage Site by Short-Range Photo-Cross-Linking[†]

Eric L. Christian,[‡] David S. McPheeters,[§] and Michael E. Harris*,[‡]

Center for RNA Molecular Biology, Departments of Molecular Biology and Microbiology and Biochemistry, Case Western Reserve University School of Medicine, Cleveland, Ohio 44106

Received August 24, 1998; Revised Manuscript Received October 5, 1998

ABSTRACT: The bacterial RNase P ribozyme is a site-specific endonuclease that catalyzes the removal of pre-tRNA leader sequences to form the 5′ end of mature tRNA. While several specific interactions between enzyme and substrate that direct this process have been determined, nucleotides on the ribozyme that interact directly with functional groups at the cleavage site are not well-defined. To identify individual nucleotides in the ribozyme that are in close proximity to the pre-tRNA cleavage site, we introduced the short-range photoaffinity cross-linking reagent 6-thioguanosine (s^6G) at position +1 of tRNA and position −1 in a tRNA bearing a one-nucleotide leader sequence [tRNA(G-1)] and examined cross-linking in representatives of the two structural classes of bacterial RNase P RNA (from *Escherichia coli* and *Bacillus subtilis*). These photoagent-modified tRNAs bind with similar high affinity to both ribozymes, and the substrate bearing a single s^6G upstream of the cleavage (−1) site is cleaved accurately. Interestingly, s^6G at position +1 of tRNA cross-links with high efficiency to homologous positions in J5/15 in both *E. coli* and *B. subtilis* RNase P RNAs, while s^6G at position −1 of tRNA(G-1) cross-links to homologous nucleotides in J18/2. Both cross-links are detected over a range of ribozyme and substrate concentrations, and importantly, ribozymes cross-linked to position −1 of tRNA(G-1) accurately cleave the covalently attached substrate. These data indicate that the conserved guanosine at the 5′ end of tRNA is adjacent to A248 (*E. coli*) of J5/15, while the base upstream of the substrate phosphate is adjacent to G332 (*E. coli*) of J18/2 and, along with available biochemical data, suggest that these nucleotides play a direct role in binding the substrate at the cleavage site.

Ribonuclease P (RNase P) catalyzes the removal of the leader sequence of pre-tRNA through an endonucleolytic cleavage to form mature tRNA. In bacteria, RNase P is composed of an RNA and a protein subunit (for recent reviews see refs *1*−*3*). The RNA subunit of RNase P can bind pre-tRNA and tRNA and catalyze the accurate cleavage of pre-tRNA in vitro (*4*). In contrast, the protein subunit of RNase P significantly enhances the ground-state binding of pre-tRNA, possibly by making contacts to the distal portion of the pre-tRNA 5′ leader sequence, but contributes only indirectly to catalysis (*5, 6*). Therefore, functional groups that direct the recognition of the pre-tRNA cleavage site reside primarily within the RNA subunit.

The secondary structure of RNase P RNA has been determined by phylogenetic comparative sequence analysis (*7*−*9*) and is composed of approximately 18 helices or paired regions (e.g., P1−P18 in *Escherichia coli*) and unpaired, or joining, sequences that connect these helices (e.g., J3/4 joins P3 with P4; Figure 1A). Although the precise secondary structure differs from organism to organism, bacterial RNase P RNAs can be divided into two distinct structural classes: type A, which is the ancestral type found in most bacteria, and type B, which occurs in the low (G + C) gram-positive bacteria (*3*; Figure 1A,B). RNase P RNAs from *E. coli* and *Bacillus subtilis* are the best-studied examples of types A and B, respectively. A number of secondary structure elements that are conserved in both classes of bacterial RNase P RNA are involved in interactions with the tRNA substrate. Several lines of evidence, including cross-linking and in vitro kinetic analyses, indicate that the T-stem and loop of tRNA are associated with the P9−11 region of the ribozyme (*10*−*12*). In addition, the 3′ CCA sequence of tRNA base-pairs with the loop, or internal bulge, of P15 (*13*−*15*). Long-range cross-linking (ca. 9 Å) with azidophenacyl (APA) reagents and chemical protection studies indicate that nucleotides in the 5′ leader sequence just upstream of the cleavage site are adjacent to the non-base-paired region J18/2 in RNase P RNA (14; Figure 1A,B), but no specific contacts between J18/2 and substrate have been defined. Similarly, long-range chemical cross-linking with APA attached to the 5′ end of tRNA identified four regions in RNase P RNA (J5/15, J18/2, L15, and J14/11) that are in the vicinity of the cleavage-site phosphate (*16*; Figure 1A,B). In these studies with APA the strongest cross-links observed were to clusters of nucleotides in J5/15, and J18/2, but specific roles for these elements in ribozyme function are not yet known. Intramolecular cross-linking studies using both *E. coli* and *B. subtilis*

[†] This work was supported by NIH Grants GM56740 to M.E.H. and GM52310 to D.S.M. E.L.C. is the recipient of an NIH postdoctoral fellowship, AI 09293. This research was supported in part by a Howard Hughes Medical Institute grant to Case Western Reserve University School of Medicine.

* Corresponding author: e-mail meh2@pop.cwru.edu.
[‡] Department of Molecular Biology and Microbiology.
[§] Department of Biochemistry.

10.1021/bi982050a CCC: $15.00
Published on Web 11/20/1998

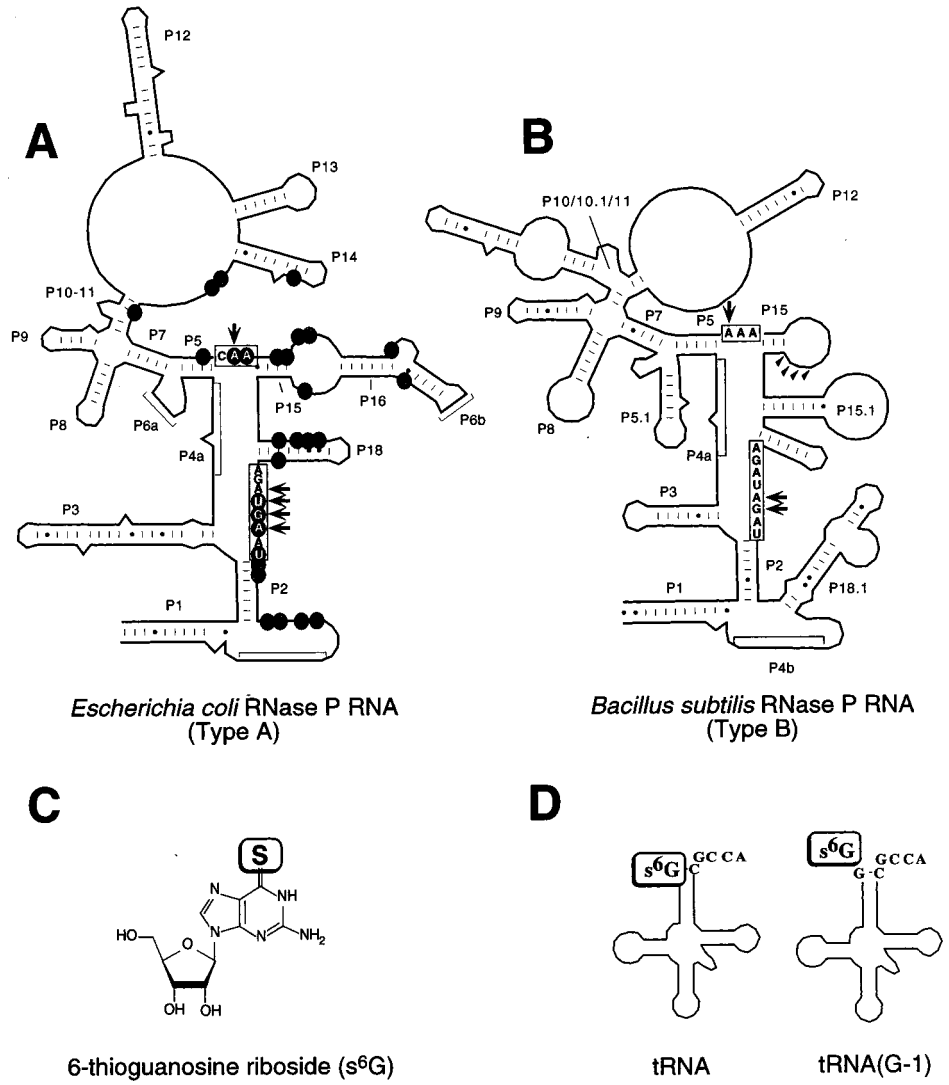

FIGURE 1: RNase P RNAs and photoagent-modified tRNAs. (**A**) *E. coli* RNase P RNA. (**B**) *B. subtilis* RNase P RNA. Nucleotides cross-linked by APA attached to the 5′ end of mature $tRNA^{Asp}$ (*16*) are indicated by arrows. s^4U cross-links from position −1 of pre-$tRNA^{His}$ (*19*) are shown as circles (major cross-links in black, minor cross-links in gray). Secondary structure regions J5/15 and J18/2 are boxed. (**C**) Cross-linking agent 6-thioguanosine (s^6G). s^6G was phosphorylated to form 6-thioguanosine 5′-monophosphate (s^6GMP), which was used to prime transcription of cross-linking substrates. (**D**) Cross-linking substrates *B. subtilis* $tRNA^{Asp}$ and *B. subtilis* $tRNA^{Asp}$ containing a single-nucleotide 5′ leader [tRNA(G-1)].

RNase P RNAs have also demonstrated that J5/15, J15/16, and J18/2 are in proximity to each other (*17*, *18*), but it is not clear whether these regions interact directly.

Recently, Kufel and Kirsebom (*19*) used 4-thiouridine (s^4U) incorporated immediately upstream of the pre-tRNA cleavage site (position −1) to demonstrate short-range cross-links to a number of different nucleotides in J5/15, J18/2, P15, and L15/16 in *E. coli* RNase P RNA (Figure 1A). In addition, minor cross-linking to several other elements of ribozyme structure was observed (Figure 1A). The large range of cross-linking sites is likely the result of multiple binding modes of the modified pre-$tRNA^{His}$ used in these experiments, which displays a significant degree of mis-cleavage by *E. coli* RNase P RNA. Although use of tRNA substrates that undergo miscleavage allows the potential identification of elements involved in cleavage site choice (*19*−*21*), it makes difficult the assignment of specific cross-links to a single native structure of the enzyme−substrate complex.

Functional groups in the nucleotides immediately upstream and downstream of the pre-tRNA cleavage site are important in cleavage site recognition. The majority of *B. subtilis* and *E. coli* tRNA genes contain a pyrimidine (usually a U) at position −1 (*22*, *23*), and changes in this nucleotide can affect both binding and catalysis (*6*, *24*−*26*). The 2′ hydroxyl of position −1 also provides an important contact for substrate binding that is likely to involve direct coordination of a metal ion required for activity (*25*, *27*). In addition, guanosine at position +1 is a highly conserved feature of *B. subtilis* (*22*) and *E. coli* tRNAs (*23*) and substitutions of this nucleotide can cause perturbation of substrate binding, catalysis, or cleavage site choice (*19*−*21*, *27*). Moreover, both nonbridging oxygens of the scissile phosphate appear to be important for cleavage by RNase P (*28*−*30*). The *pro-*R_p oxygen, in particular, coordinates a magnesium ion that is important for catalysis (*29*−*30*). Despite this information, nucleotides in RNase P RNA that interact with the functional groups of the substrate adjacent to the cleavage site have not been clearly identified. While it is likely that the functional groups in nucleotides at positions +1 and −1 of the pre-tRNA substrate interact with J5/15, J18/2, or J15/16 in RNase P RNA, the identification of specific contacts

remains an important goal in understanding cleavage site recognition.

To identify individual nucleotides in RNase P RNA that may be involved in recognition of the residues adjacent to the pre-tRNA cleavage site, we positioned the short-range photoaffinity cross-linking reagent 6-thioguanosine (s^6G; Figure 1C) at the 5′ ends of mature *B. subtilis* $tRNA^{Asp}$ (tRNA) and *B. subtilis* $tRNA^{Asp}$ bearing a single-nucleotide leader sequence [tRNA(G-1); Figure 1D]. We find that both tRNA and tRNA(G-1) are bound by *E. coli* and *B. subtilis* RNase P RNAs with high affinity and that tRNA(G-1) is cleaved accurately and efficiently by both ribozymes. We also find that photoagents at positions −1 and +1 cross-link to different elements of RNase P RNA structure but detect homologous nucleotides in both the *E. coli* and *B. subtilis* ribozymes. These data indicate that the nucleotide upstream of the substrate phosphate is adjacent to the nucleotide position homologous to G332 (*E. coli*) of J18/2, while the mature tRNA 5′ end is adjacent to the nucleotide homologous to A248 (*E. coli*) of J5/15 in bacterial RNase P RNA.

MATERIALS AND METHODS

Preparation of 6-Thioguanosine 5′-Monophosphate. To incorporate s^6G during transcription reactions, it was necessary to use the 5′-monophosphate derivative of s^6G to increase the solubility of this compound. 6-Mercaptoguanosine (2 mmol, Sigma) was dissolved in 5.0 mL of triethyl phosphate and stirred on ice for 10 min. Phosphoryl chloride (0.6 mL, 5.8 mmol, Aldrich) was then added and the mixture was stirred on ice in the dark for 4 h to yield a clear yellow solution. After the volume was adjusted to 500 mL with ice-cold water, the pH was adjusted to ∼7.5 by the addition of triethylamine (∼4.1 mL) over a period of 2 h. The neutralized reaction mixture was then loaded onto a 2.5 cm × 18 cm TSK-gel Toyopearl DEAE-650M column (Supelco) previously equilibrated with 0.05 M triethylammonium bicarbonate (pH 7.5) at a flow rate of 60 mL/h, and the column was washed with 4 volumes of 0.05 M triethylammonium bicarbonate (pH 7.5). 6-Thioguanosine 5′-monophosphate (s^6GMP) was eluted with a 400 mL linear gradient of 0.05−0.5 M triethylammonium bicarbonate (pH 7.5). Fractions containing s^6GMP were located by measuring the absorption at 252 nm after a 200-fold dilution into 1 mM sodium hydroxide. Peak fractions were subsequently pooled, and the buffer was removed by vacuum with the addition of 3 × 50 mL methanol. Solid s^6GMP (0.2 mmol) was then dissolved in water at a final concentration of ∼50 mM, the pH was adjusted to ∼7 with NaOH, and the solution was stored in the dark at −70 °C. The ^1H NMR spectrum of the final product was found to be consistent with published values (*31*). The UV spectrum (220−360 nm) measured for the final product (diluted in 1.0 mM NaOH) was also found to be identical to that of the starting material, indicating that the thio group was not lost during the procedure.

Preparation of RNA. RNase P RNAs and modified tRNAs used in this study were generated by in vitro transcription from linearized plasmids with T7 RNA polymerase. Specifically, *E. coli* RNase P RNA was transcribed from pDW98 (see below) digested with *Sna*BI, and *B. subtilis* RNase P RNA was transcribed from pDW66 (see below) digested with *Dra*I. Mature $tRNA^{Asp}$ from *B. subtilis*, or mature *B. subtilis* $tRNA^{Asp}$ with a single-nucleotide 5′ leader, referred to as tRNA(G-1) (see Figure 1), were transcribed from plasmids pMBSD or pBJ1 respectively, after digestion with *Bst*NI. With the exception of pBJ1, these plasmids were generous gifts from the laboratory of Dr. Norman R. Pace. Transcription of RNase P RNAs was carried out in a volume of 100 μL in a reaction mixture containing 2 μg of plasmid DNA, 1 mM rNTPs, 40 mM Tris-HCl, pH 7.9, 6 mM $MgCl_2$, 2 mM spermidine, and 10 mM dithiothreitol and were incubated for 6−14 h at 37 °C. To incorporate s^6GMP at the 5′ ends of either tRNA or tRNA(G-1), the reactions were modified to contain 0.1 mM GTP and 1.6 mM s^6GMP. Transcription reactions for generation of uniformly labeled RNAs were supplemented with 200 μCi of [α-^{32}P]GTP. Reactions were terminated by dilution to 200 μL with 10 mM Tris-HCl, pH 8.0, and 1 mM EDTA, followed by precipition with 0.3 M sodium acetate and 3 volumes of ethanol, and purification on 4% (RNase P RNA) or 6% (tRNA) (19:1) polyacrylamide gels. RNA products were visualized by brief UV (254 nm) shadowing, and RNAs were eluted from the excised gel slices in 4 volumes (usually 400 μL) of 40 mM Tris-HCl, pH 8.0, 1 mM EDTA, 0.3 M sodium acetate, and 0.1% sodium dodecyl sulfate (SDS) for 4−12 h. Eluted RNAs were extracted twice with an equal volume of a 1:1 mixture of phenol and chloroform and once with an equal volume of chloroform and then precipitated with 3 volumes of ethanol. The amount of RNA was determined by measuring absorbance at 260 nm or calculated from the specific activity of incorporated radioactive nucleotide. tRNA and tRNA(G-1) (20 pmol) were 5′-end-labeled for kinetic and cross-linking studies with 150 μCi of [γ-^{32}P]-ATP (New England Nuclear) and T4 polynucleotide kinase (Life Technologies) with exchange reaction buffers from the vendor and were purified as described above.

Determination of K_D and k_{app} and the Accuracy of tRNA-(G-1) Cleavage. The affinity of tRNA and tRNA(G-1) for both *E. coli* and *B. subtilis* RNase P RNA was measured by gel filtration by using a method adapted from Beebe and Fierke (*32*). Chromatography on G-75 Sephadex can be used to measure the fraction of substrate bound to enzyme because free tRNA [and tRNA(G-1)] are partitioned between included and excluded volumes, whereas enzyme−substrate complexes are sufficiently large to be excluded, and elute in the void volume. RNase P RNA and 5′-^{32}P-end-labeled tRNA or tRNA(G-1) were renatured separately in the presence of 2 M ammonium acetate, 50 mM Tris-HCl, pH 8.0 and 25 mM calcium chloride by incubation at 65 °C for 90 s followed by incubation at 37 °C for 15 min. 5′-^{32}P-End-labeled tRNA or tRNA(G-1) was then combined with *E. coli* or *B. subtilis* RNase P RNA at concentrations indicated in Figure 2 and incubated for 2 min at 37 °C before being added to spin columns containing 0.6 mL of packed G75 Sephadex in 2 M ammonium acetate, 40 mM Tris-HCl, pH 8.0, 25 mM calcium chloride, and 0.5% NP-40. Columns were spun for 2 min at 2500*g*. Ribozyme−substrate complexes detected in the flowthrough were subsequently recovered, and the amount of bound RNA was determined by Cerenkov scintillation counting. The fraction of bound substrate ([E−S]) was fit to

$$[E-S]/[E-S]_{\infty} = 1/\{1 + (K_D/[E])\} \quad (1)$$

where [E−S] is the amount of radioactivity recovered in the bound fraction, $[E-S]_{\infty}$ is the maximum amount of bound radioactivity recovered at the end point of the reaction, and [E] is the concentration of ribozyme in the binding reaction.

The apparent cleavage rate, k_{app}, for a single-turnover reaction under conditions of excess enzyme ([E]/[S] > 5) was determined at pH 6.0 to suppress the cleavage rate so that time points could be collected manually (*25*). Cleavage of 5′-^{32}P-end-labeled tRNA(G-1) substrate (2.5 nM) was measured at high concentrations of RNase P (125−500 nM) identified to be saturating with respect to substrate. k_{app} is thus a close approximation to the rate constant k_2, which describes the rate of cleavage of the bound substrate. Specifically, *E. coli* or *B. subtilis* RNase P RNA and tRNA(G-1) were resuspended separately in 2 M NH_4Cl and 40 mM PIPES (pH 6.0) and heated at 95 °C for 3 min, followed by the addition of $MgCl_2$ to 25 mM and further incubated at 37 °C for 15 min. Reactions (20 μL) were initiated by mixing ribozyme and substrate, and incubating at 37 °C for 5−180 s (*E. coli* RNase P RNA) or 1−30 min (*B. subtilis* RNase P RNA). Aliquots (2 μL) of the reaction were taken at times indicated in Figure 3A,B and the reactions were terminated by addition of 100 mM EDTA (4 μL). Reaction products were resolved by one-dimensional thin-layer chromatography on polyethylenimine cellulose (Aldrich) in 66:33:1:1 (v/v/v/v) isobutyric acid/water/ammonium hydroxide/0.5 M EDTA (*33*) and quantified with a Molecular Dynamics phosphorimager. Reaction rates were obtained by plotting the fraction substrate cleaved versus time and fitting the data to an expression for single-exponential decay:

$$[P]/[S]_{total} = A - B(e^{-kt}) \quad (2)$$

where [P] is the amount of product measured, $[S]_{total}$ is the total amount of substrate added to the reaction, *A* is the maximal extent of reaction, and *B* is the amplitude of the exponential (*34*).

The accuracy of *E. coli* and *B. subtilis* RNase P RNA cleavage of 5′-^{32}P-end-labeled tRNA(G-1) containing s^6GMP at its 5′ end was examined by resolving cleavage products by two-dimensional thin-layer chromatography. Cleavage reaction products along with 5′-AMP, 5′-CMP, 5′-GMP, and 5′-UMP (Sigma) and s^6GMP standards were separated on polyethylenimine cellulose in 66:33:1:1 (v/v/v/v) isobutyric acid/water/ammonium hydroxide/0.5 M EDTA as described above, dried for 1 h at room temperature, and resolved in the second dimension in 70:20:15:1 (v/v/v/v) 2-propanol/water/concentrated HCl/0.5 M EDTA. TLC plates were then dried overnight in a fume hood at room temperature. Positions of the standards were determined by UV shadowing (254 nm) with a hand-held UV lamp (UVP, model UVGL-58, Upland, Ca) and aligned with the position of the ^{32}P-labeled tRNA(G-1) cleavage product on an autoradiograph with the aid of fluorescent markers (Stratagene).

Cross-Linking of 5′ s^6G-Modified tRNA and tRNA(G-1) to RNase P RNA. Cross-linking of 5′-^{32}P-end-labeled tRNA or tRNA(G-1), containing s^6G at their 5′ ends, to either *E. coli* or *B. subtilis* RNase P RNA was performed under conditions of enzyme excess ([E]/[S] = 10) in the presence of calcium ions on ice to suppress cleavage of the cross-linking substrate. These conditions were found to give the highest yield of cross-linked products [identical cross-links are also observed at higher temperatures under these conditions (data not shown)]. Specifically, 100 nM tRNA or tRNA(G-1) and 1 μM *E. coli* or *B. subtilis* RNase P RNA were resuspended separately in 2 M ammonium acetate and 50 mM Tris-HCl, pH 8.0, and heated to 95 °C for 3 min. $CaCl_2$ was then added to a final concentration of 25 mM and the sample was incubated at 37 °C for 15 min. Equal volumes of tRNA or tRNA(G-1) and ribozyme were then mixed and incubated for an additional 2 min at 37 °C to allow the cross-linking substrate to bind to the ribozyme and then set on ice. For analytical reactions (Figure 4), aliquots (12 μL) were transferred to a parafilm-covered aluminum block on ice and irradiated for 15 min at 366 nm (UVP, model UVGL-58, Upland, CA) through a 1/8 in. standard glass plate at a distance of 3 cm (*16*). Aliquots were then phenol- and chloroform-extracted, ethanol-precipitated, and gel-purified as described above. For preparative-scale cross-linking reactions used in primer extension mapping (Figure 5, see below), 500 μL reactions were irradiated in 12 μL aliquots, pooled, and purified as described above. Both reactions contained a final concentration of 40 nM cross-linking substrate and 400 nM ribozyme.

The sites of cross-linking within *E. coli* or *B. subtilis* RNase P RNA were determined by primer extension sequencing adapted from Burgin and Pace (*16*). Equal amounts of gel-purified cross-linked material and 5′-^{32}P-end-labeled sequencing primers (usually 0.1−0.2 pmol each in 5 μL) were incubated at 65 °C for 3 min in 50 mM Tris-HCl (pH 8.3), 15 mM NaCl, and 10 mM DTT and then frozen immediately on dry ice. Samples were then thawed on ice, and $MgCl_2$ (1 μL) was added to a final concentration of 6 mM. All four deoxynucleotides (dATP, dCTP, dGTP, and dTTP) and 2 units of AMV reverse transcriptase (Boehringer Mannheim) were subsequently added to the samples (to a final volume of 10 μL), which were then incubated at 47 °C for 5 min. Reactions were terminated with the addition of an equal volume of 0.5 M NaCl, 20 mM EDTA, and 5 μg of glycogen (Boehringer Mannheim) and precipitated with 2.5 volumes (50 μL) of ethanol. Reactions were resuspended in 2 μL of dH_2O and 2 μL of loading buffer containing 95% formamide, 150 mM Tris-HCl (pH 8.0), 15 mM EDTA, and 1 mg/mL bromophenol blue and xylene cyanol FF. Samples were heated to 95 °C for 3 min, set on ice for 2 min, and separated on a 6% polyacrylamide gel next to standard dideoxy sequencing reactions containing un-cross-linked *E. coli* or *B. subtilis* RNase P RNA, 0.5 mM dideoxynucleotides under the conditions above.

The formation of cross-links was determined to be relatively slow (<1/min, data not shown) and therefore assumed to be slower than the dissociation of the native enzyme−tRNA complex. Thus, the amount of cross-link formed after a fixed time reflects the concentration of enzyme−tRNA complexes in solution. To determine an apparent K_D by cross-linking, the amount of cross-linked product formed was measured over a range of *E. coli* or *B. subtilis* RNase P RNA concentrations where [E]/[S] > 5 and [S] = 0.05−2.5 nM. For tRNA, [E] = 0.1−100 nM, and for tRNA(G-1), [E] = 1−100 nM. Cross-linking was performed as described above and the amount of cross-linked

product formed was quantified with a Molecular Dynamics phosphorimager. K_{Dapp} was derived by plotting the fraction of substrate cross-linked versus ribozyme concentration and fitting the data to eq 1.

The catalytic activity of cross-linked complexes of tRNA(G-1) and *E. coli* or *B. subtilis* RNase P RNAs was determined by incubating the analytical cross-linking reactions described above under conditions that promote pre-tRNA cleavage by RNase P RNA. Specifically, after analytical cross-linking, reactions were combined with $MgCl_2$ and EGTA to a final concentration of 25 mM each in 2 M ammonium acetate and 50 mM Tris-HCl, pH 8.0. The reaction mixture was then incubated for 60 min at 37 °C, and the reaction products were phenol-extracted, ethanol-precipitated, and separated on a 6% polyacrylamide gel as described above. Alternatively, gel-purified cross-linked material (approximately 0.1−0.2 pmol in 16 μL) was incubated for 60 min at 37 °C in 2 M ammonium acetate, 25 mM $MgCl_2$, and 50 mM Tris-HCl, pH 8.0, and purified and analyzed as above.

RESULTS

tRNA and tRNA(G-1) Bind with High Affinity to both the E. coli and B. subtilis Ribozymes. Several lines of evidence indicate that the major determinants on the pre-tRNA substrate for binding and cleavage reside within the mature tRNA. First, tRNA is a competitive inhibitor of the in vitro cleavage reaction, indicating that the binding sites for precursor and product are overlapping (*35*). Second, the binding of both tRNA and pre-tRNA substrate protect nearly the same set of nucleotides from chemical modification. The only exceptions are G332 and A333 (*E. coli*) in J18/2, which are uniquely altered in their chemical modification patterns by pre-tRNA (*14*; see below). Third, a pre-tRNA with only a single nucleotide upstream of the cleavage site shows little perturbation in binding or catalyis by *E. coli* RNase P RNA in vitro (*25*). In fact, bacterial pre-tRNAs containing 5′ leader sequences as short as two nucleotides occur in vivo (*22*, *23*). Short-range cross-linking from bases adjacent to the cleavage site in the context of tRNA and a substrate containing a single nucleotide leader upstream of the cleavage site should, therefore, be highly analogous with respect to their interaction with the ribozyme and should reveal nucleotides in RNase P RNA adjacent to the substrate phosphate.

To determine the relative affinity of the ribozyme for our tRNA and tRNA(G-1) photoaffinity probes, we initially examined the binding of these RNAs to *E. coli* and *B. subtilis* RNase P ribozymes by using gel filtration (*32*, *36*, *37*). Figure 2 shows the amount of tRNA and tRNA(G-1) bound over a range of *E. coli* and *B. subtilis* RNase P RNA concentrations. Both tRNAs are bound with high affinity by the ribozymes, as reflected in equilibrium binding constants of less than 2 nM for tRNA and less than 5 nM for tRNA(G-1) (Table 1). The moderate increase in K_D for tRNA(G-1) relative to tRNA indicates that the presence of a single nucleotide just upstream of the cleavage site results in a small destabilization of the ground-state complex ($\Delta\Delta G$ < 0.5 kcal/mol). The dissociation constants for $tRNA^{Asp}$ are essentially identical to that observed previously under somewhat lower monovalent salt conditions [2.1 nM for *B. subtilis* RNase P RNA in 1 M NH_4Cl (*6*)]. Interestingly, however, the dissociation constant for a tRNA with a single nucleotide leader is significantly lower in the presence of higher levels of monovalent salt used in the current study (4.5 nM vs 40 nM for 2 M NH_4Cl and 1 M NH_4Cl, respectively; Table 1, and ref *6*). These data suggest that the increase in ionic strength acts to specifically stabilize the nucleotide at position −1 in the ribozyme−substrate complex.

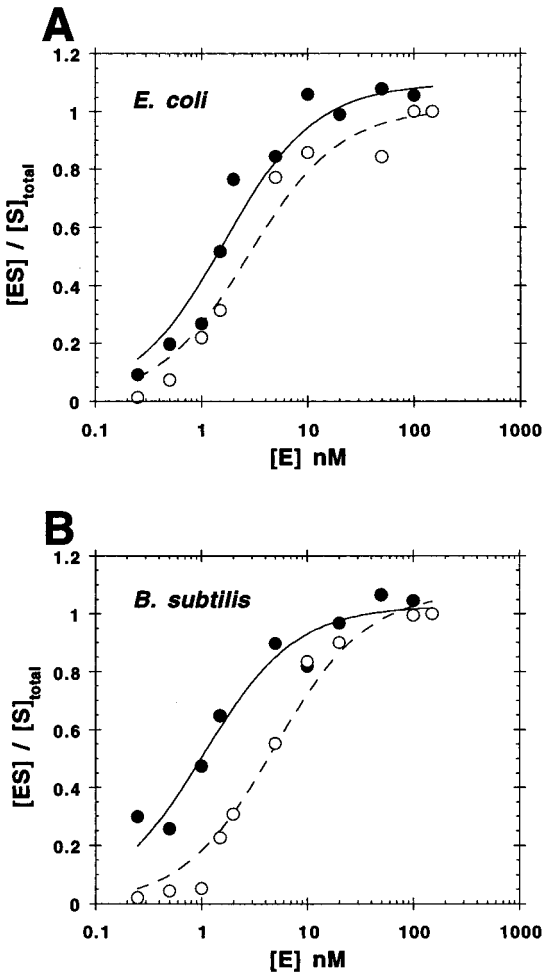

FIGURE 2: Binding of tRNA and tRNA(G-1) by *E. coli* and *B. subtilis* ribozymes. (**A**) tRNA and tRNA(G-1) binding by *E. coli* RNase P RNA. (**B**) tRNA and tRNA(G-1) binding by *B. subtilis* RNase P RNA. 5′-End-labeled cross-linking substrate (S) (0.02−2.5 nM) was incubated in excess *E. coli* or *B. subtilis* ribozyme (E) ([E]/[S] > 5) in 40 mM Tris, 25 mM $CaCl_2$, 2 M $NH_4C_2H_3O_2$, and 0.01% NP40 (pH 8.0) and spun through a 1 mL Sephadex G-75 column to separate unbound substrate from substrate bound to ribozyme [E−S]. The level of bound substrate was determined by scintillation counting and plotted as a fraction of total substrate $[S]_{total}$ versus enzyme concentration. For tRNA, [E] = 0.25−100 nM, and for tRNA(G-1), [E] = 0.25−125 nM. The dissociation constant (K_D) was determined from a fit of the data to eq 1. (●) Binding data for tRNA; (○) binding data for tRNA(G-1).

In addition to binding, the rate of cleavage (k_{app}) of the bound s^6G-modified tRNA(G-1) substrate by *E. coli* and *B. subtilis* RNase P RNAs was also measured (Figure 3A,B). In these kinetic experiments the concentration of enzyme was kept well above (>25-fold) the measured K_D. Under these conditions the reaction rate reflects the rate of cleavage of the bound substrate for *B. subtilis* RNase P RNA and is presumably the same for the *E. coli* ribozyme (*5*, *6*, *32*). These experiments were performed at pH 6.0 to slow the reaction rate to allow the kinetic values to be determined

Table 1: Kinetic Parameters for tRNA, tRNA(G-1), and Pre-tRNA

	E. coli			*B. subtilis*		
	K_D (nM) (gel filtration[a])	K_D (nM) (x-linking[b])	k_{app} (min^{-1}) (single turnover)	K_D (nM) (gel filtration[a])	K_D (nM) (x-linking[b])	k_{app} (min^{-1}) (single turnover)
tRNA	1.5 ± 0.4	1.3 ± 1.2	n/a	1.8 ± 0.6	1.5 ± 1.6	n/a
tRNA(G-1)	3.2 ± 0.7	5.8 ± 2.5	2.5 ± 0.3[c]	4.5 ± 0.9	4.0 ± 2.2	0.38 ± 0.04[c]
pre-tRNA	34 ± 4	n/a	2.2 ± 0.1[d]	42 ± 2	n/a	1.3 ± 0.8[d]

[a] Determined by gel filtration on G-75 Sephadex in 2 M ammonium acetate, 50 mM Tris-HCl, pH 8.0, 25 mM calcium chloride, and 0.01% NP-40. [b] Determined by photo-cross-linking in 2 M ammonium acetate, 50 mM Tris-HCl, pH 8.0, 25 mM calcium chloride, and 0.01% SDS. [c,d] Single-turnover cleavage rate was measured with 0.5 nM substrate and 0.5−2 μM ribozyme in 2 M ammonium acetate (*c*) or 1 M ammonium acetate (*d*) plus 50 mM PIPES, pH 6.0, 25 mM magnesium chloride, and 0.01% SDS.

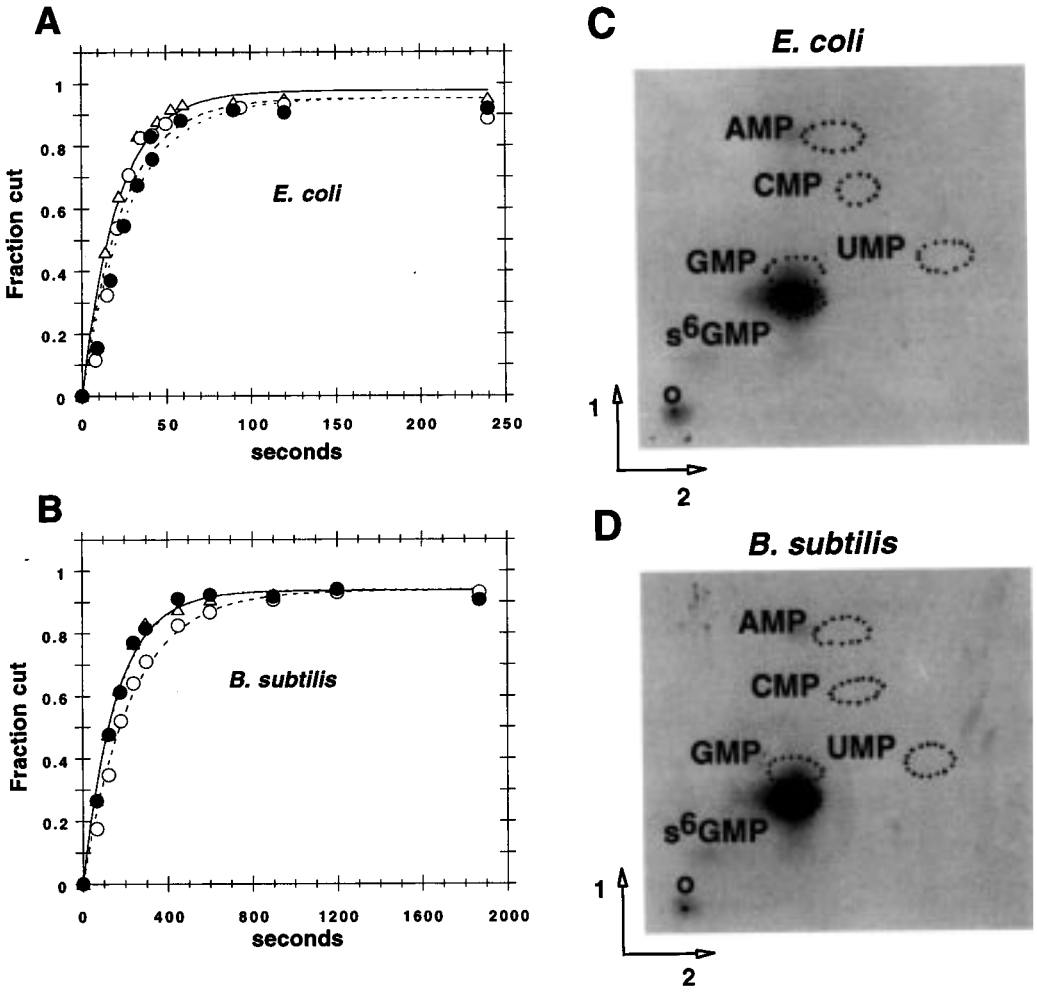

FIGURE 3: Rate and accuracy of tRNA(G-1) cleavage. (k_{app}) for tRNA(G-1) (S) was determined from single-turnover kinetics in 40 mM PIPES, 25 mM $MgCl_2$, 2 M NH_4Cl, and 0.01% SDS (pH 6.0) at saturating concentrations of enzyme (E) (where [E]/[S] > 50; [S] = 2.5 nM) for both *E. coli* RNase P RNA (**A**) and *B. subtilis* RNase P RNA (**B**). For each [E], 125 nM (●), 250 nM (○) and 500 nM (△), the fraction of substrate cleaved was plotted against time and the data were fit to a single-exponential decay to obtain k_{app} (eq 2). The accuracy of *E. coli* (**C**) and *B. subtilis* (**D**) RNase P RNA cleavage of 5′-^{32}P-end-labeled tRNA(G-1) was examined by resolving cleavage products by two-dimensional thin-layer chromatography. The positions of unlabeled nucleotide standards 5′-AMP, 5′-CMP, 5′-GMP, 5′-UMP, and 5′-s^{6}GMP were determined by UV shadowing and aligned with an autoradiograph of the ^{32}P-end-labeled cleavage product. A lowercase o denotes the position where samples were originally spotted. Numbers and arrows indicate direction of the first or second dimension of the chromatographic analysis.

manually. This diffence in pH is not likely to alter the structure of the enzyme−substrate complex significantly, given that pH changes have been shown to have little effect on binding between pH 6 and 8 (*25*) and are likely to be further muted under the current conditions of enzyme saturation. We find that, as expected, the k_{app} for tRNA(G-1) cleavage is essentially constant over the range of excess RNase P RNA concentrations used (125−500 nM), suggesting that the enzyme is saturating and that the observed rate (averaged in Table 1) approximates the catalytic rate constant k_2. The k_{app} under single-turnover conditions for tRNA(G-1) cleavage by *E. coli* RNase P RNA is essentially the same as that observed for pre-tRNA containing a complete leader sequence, while the observed rate constant for tRNA(G-1) cleavage by *B. subtilis* RNase P is decreased by less than 4-fold (Table 1). These results show that the binding of tRNA and tRNA(G-1) occurs with nearly equal affinity and that the tRNA(G-1) substrate is cleaved by both

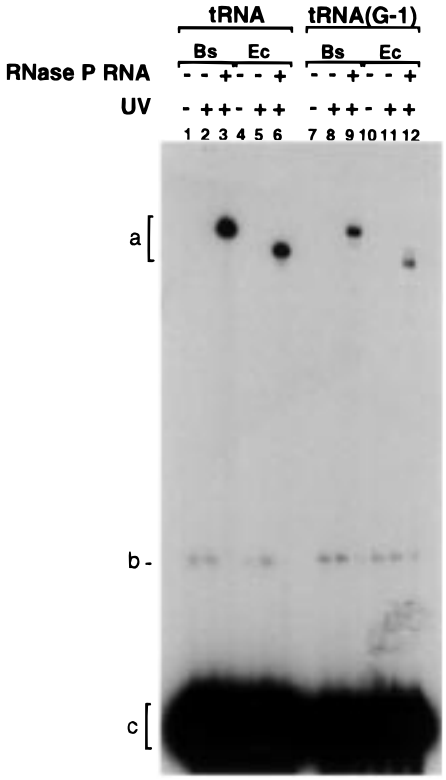

FIGURE 4: Intermolecular cross-linking to RNase P RNA. 5′-^{32}P-end-labeled tRNA (lanes 1−6) or tRNA(G-1) (lanes 7−12) containing s^{6}G at their 5′ ends were cross-linked to *B. subtilis* (Bs) RNase P RNA (lanes 3 and 9) or *E. coli* (Ec) RNase P RNA (lanes 6 and 12) in the presence of UV light in 50 mM Tris, 25 mM $CaCl_2$, 2 M $NH_4C_2H_3O_2$, and 0.01% SDS (pH 8.0) on ice under conditions of enzyme excess ([E]/[S] = 10). The same cross-links are observed at higher temperatures but with higher levels of substrate cleavage (data not shown). No cross-linking was observed in samples lacking either UV light (lanes 1, 4, 7, and 10) or ribozyme (lanes 1, 2, 4, 5, 7, 8, 10, and 11). (**a**) Intermolecular tRNA or tRNA(G-1) cross-links with RNase P; (**b**) intramolecular tRNA or tRNA(G-1) cross-links; (**c**) uncross-linked tRNA or tRNA(G-1).

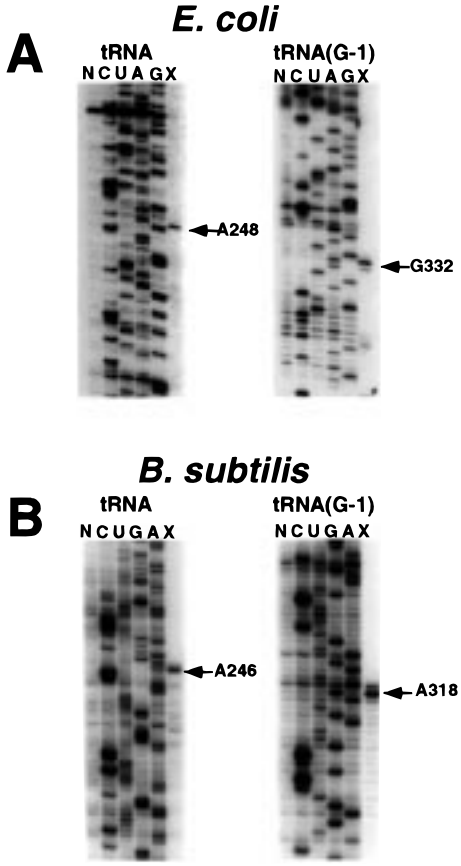

FIGURE 5: Primer extension mapping of intermolecular cross-links. Lanes C, U, A, and G reflect a standard dideoxy sequencing reaction of uncross-linked *E. coli* RNase P RNA (panel **A**) or *B. subtilis* RNase P RNA (panel **B**). Lane N reflects sequencing reaction containing no dideoxy nucleotides to control for reverse transcriptase stops caused by ribozyme structure. Lane X reflects primer extension reactions of gel-purified intermolecular cross-links containing tRNA (left) or tRNA(G-1) (right). Arrow indicates position of principal cross-link. Aside from minor cross-links adjacent to the indicated positions no other cross-links are observed.

ribozymes at essentially the same rate as that observed for pre-tRNAs with longer leader sequences.

Substrates with alterations at the cleavage site can undergo miscleavage in both the 5′ leader and mature tRNA sequences (*38*−*40*). To examine the accuracy of tRNA(G-1) cleavage by both *E. coli* and *B. subtilis* RNase P RNAs, reaction products were analyzed by two-dimensional thin-layer chromatography (Figure 3C,D). We find that essentially all of the tRNA(G-1) cleavage product comigrates with the s^{6}GMP standard, demonstrating that the tRNA(G-1) substrate is cleaved accurately by both ribozymes, and that the accuracy of cleavage is not perturbed by the presence of the cross-linking agent. Moreover, the absence of significant levels of cleavage product comigrating with GMP indicates that the cleaved substrate is efficiently modified with s^{6}GMP and that little, if any, oxidation of the 6-thio group had occurred during sample preparation. Taken together, these results show that the presence of a single-nucleotide leader results in only a slight effect on binding and cleavage by the ribozyme.

Site-Specific Photo-Cross-Linking to RNase P RNA. Cross-linking of tRNA and tRNA(G-1) to *E. coli* and *B. subtilis* RNase P RNA was performed under conditions of excess enzyme ([E]/[S] = 10) and in the presence of $CaCl_2$ (25 mM) to suppress cleavage of tRNA(G-1) substrate. Substitution of magnesium ion by calcium inhibits the rate of pre-tRNA cleavage approximately 10^4-fold (*25*, *41*), with little perturbation of the structure of the enzyme−substrate complex as judged by intramolecular cross-linking (*42*). Cross-links formed under these conditions are, therefore, likely to be indicative of structural features of ground-state binding rather than structural features related to catalysis or the transition state. Irradiation of 5′-s^{6}G-modified tRNA and tRNA(G-1) in the presence of either *E. coli* or *B. subtilis* RNase P RNAs results in the formation of a single high-efficiency intermolecular cross-link band for each pairwise combination of ribozyme and cross-linking substrate (Figure 4). Formation of these cross-links is dependent upon UV irradiation and the presence of RNase P RNA (Figure 4) and is not observed with unmodified tRNA or tRNA(G-1) (data not shown).

To confirm the presence of RNase P RNA in the cross-linked bands and to determine the identity of the cross-linked nucleotides, individual cross-linked species were isolated by gel purification and the sites of cross-linking were mapped by primer extension with reverse transcriptase. Reverse transcriptase terminates on RNA templates one nucleotide upstream of the cross-linked nucleotides (*43*), and thus, comparison of the extension products obtained with cross-linked RNAs to those generated with un-cross-linked RNAs

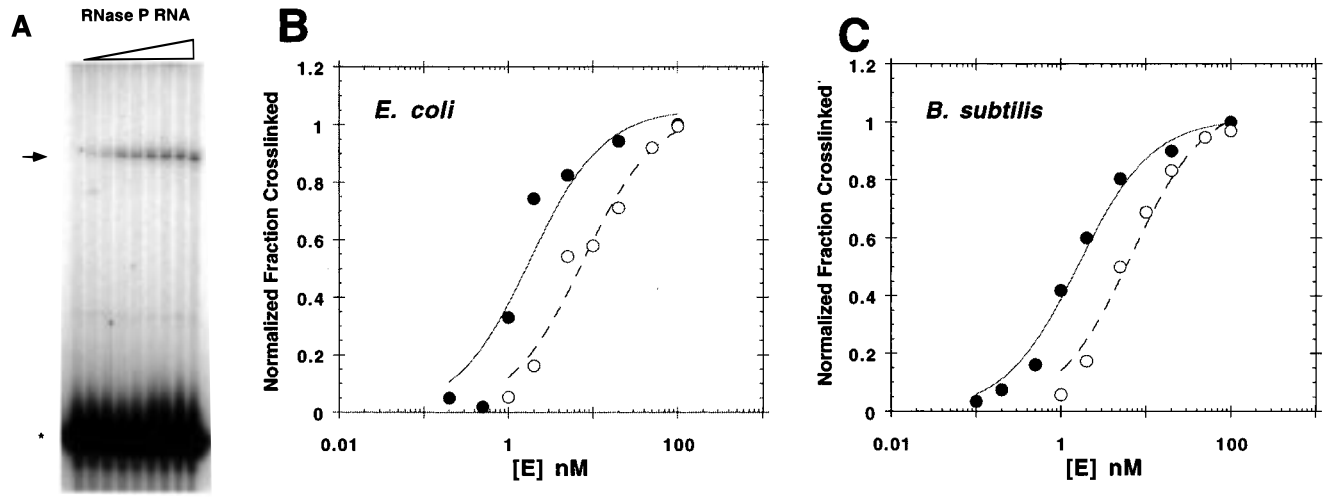

FIGURE 6: Measurement of dissociation constant (K_{Dapp}) by cross-linking. 5′-^{32}P-End-labeled tRNA or tRNA(G-1) containing s^{6}G at their 5′ ends were cross-linked to *B. subtilis* RNase P RNA or *E. coli* RNase P RNA under buffer conditions described in Figure 4 over a range of enzyme concentrations in which enzyme is kept in excess ([E]/[S] > 5 with [S] = 0.05−2.5 nM). For tRNA, [E] = 0.1−100 nM, and for tRNA(G-1), [E] = 1−100 nM. (**A**) Example of tRNA cross-linking to *E. coli* RNase P RNA. Arrow indicates a position of intermolecular cross-linking; asterisk indicates the position of tRNA. (**B**, **C**) Normalized fractions of tRNA (●) or tRNA(G-1) (○) cross-linking plotted versus *E. coli* RNase P RNA (**B**) or *B. subtilis* RNase P RNA (**C**) concentration. K_{Dapp} was calculated from a fit to eq 1.

and sequencing standards identifies the individual cross-linked nucleotides (Figure 5). Primer extensions of cross-linked species containing 5′-s^{6}G-modified tRNA terminated in the J5/15 region of both *E. coli* and *B. subtilis* RNase P RNAs. Interestingly, these cross-links occur at homologous nucleotide positions in both ribozymes: A248 in the *E. coli* RNase P RNA and A246 in *B. subtilis* RNase P RNA (Figures 5 and 8). Positioning s^{6}G one nucleotide upstream of the cleavage site in tRNA(G-1), however, produces cross-links to a different region in these ribozymes. Here, no cross-linking was detected to J5/15, but strong reverse transcriptase terminations were detected in J18/2. Again, homologous nucleotides were detected in each of the ribozymes: G332 (with minor cross-linking to A333) in *E. coli* RNase P RNA and A318 (with minor cross-links to U317 and G319) in *B. subtilis* RNase P RNA.

Because preparative cross-linking was performed under conditions of enzyme excess (10× K_D) in order to obtain sufficient material for analysis, it is possible that the resulting cross-linked species could reflect non-native, low-affinity complexes of enzyme and substrate. Conversely, if the cross-links above are the result of native, high-affinity ribozyme−tRNA complex formation, then the amount of cross-linked material should be directly proportional to the concentration of enzyme−substrate complex as measured by other means. Accordingly, we analyzed cross-linking of tRNA and tRNA-(G-1) over a range of concentrations of either *E. coli* or *B. subtilis* RNase P RNA. Figure 6A shows a representative cross-linking result with tRNA and *E. coli* RNase P RNA. Data for each of the four pairwise combinations of cross-linking substrate and ribozyme are plotted in Figure 6B,C and summarized in Table 1. Each of the cross-linked species was detected at very low (1 nM) concentrations of ribozyme and increased with increasing concentrations of ribozyme, reaching saturation between 20 and 50 nM. Fitting the cross-linking data above to a simple binding isotherm (eq 1) allows calculation of an apparent K_D for binding of tRNA and tRNA(G-1) to the *E. coli* and *B. subtilis* ribozymes (Figure 6B and Table 1). Apparent K_D values of 1.3 nM for tRNA and 5.8 nM for tRNA(G-1) were obtained for the *E. coli* ribozyme and found to be similar to K_D values of 1.5 nM for tRNA and 4 nM for tRNA(G-1) obtained for the *B. subtilis* RNase P RNA. The apparent K_D values from the cross-linking assay are in good agreement with the values obtained from the gel-filtration assay (Table 1). These data are again consistent with the formation of high-affinity complexes between the ribozyme and cross-linking substrate and suggest that the cross-links reflect the native enzyme−tRNA complex.

Intermolecular Cross-Links between tRNA(G-1) and RNase P RNA Retain Catalytic Activity. A crucial test of whether the observed cross-links reflect the native enzyme structure is to determine whether the cross-linked species retain catalytic activity. Since the cross-links between RNase P RNA and tRNA join ribozyme and product, it is not possible to assess the catalytic activity of these complexes. Cross-links between RNase P RNA and tRNA(G-1), however, may still retain the ability to hydrolyze the phosphodiester bond between the one-nucleotide leader sequence, now covalently attached to the ribozyme, and the mature tRNA. To assess the ability of the cross-linked conjugates to cleave the attached substrate, we generated cross-linked conjugates containing nonradiolabeled RNase P RNA and 5′-end-labeled tRNA(G-1) as described above. After cross-linking, magnesium was added to accelerate the RNase P-catalyzed hydrolysis reaction. Cleavage of the attached substrate should release the mature tRNA fragment, but the 5′ radiolabeled s^{6}G single-nucleotide leader should remain covalently attached to the ribozyme and should be visible as a radiolabeled species that comigrates with linear RNase P RNA.

Figure 7 shows the results of this analysis for intermolecular cross-linking between tRNA(G-1) and both the *E. coli* and *B. subtilis* RNase P ribozymes. As shown previously (Figure 4), UV irradiation of complexes of 5′-s^{6}G-modified tRNA(G-1) and RNase P RNA formed in the presence of calcium results in a single high-efficiency intermolecular cross-link species that migrates at approximately 622 nucleotides for *B. subtilis* RNase P RNA and a species of approximately 540 nucleotides for *E. coli* RNase P RNA. Addition of magnesium to the reaction results in conversion

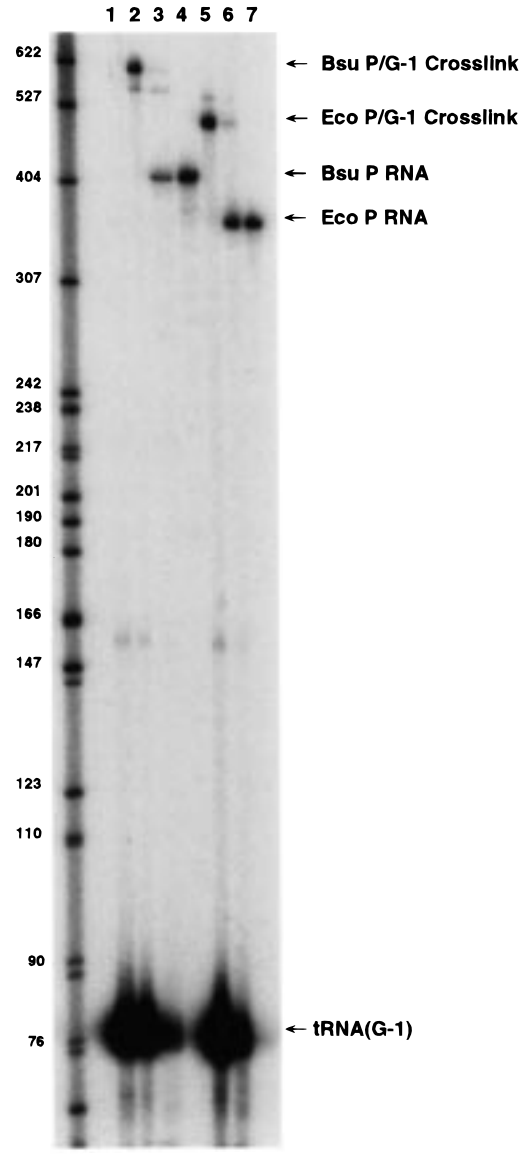

FIGURE 7: Catalytic activity of tRNA(G-1) cross-links. 5′-^{32}P-End-labeled tRNA(G-1) containing s^6G at its 5′ ends (lane 1) was cross-linked to *B. subtilis* RNase P RNA (lane 2) or *E. coli* RNase P RNA (lane 5) as described in Figure 4. Samples were subsequently incubated with magnesium to accelerate the RNase P-catalyzed hydrolysis reaction and found to produce cross-linked species (*B. subtilis*, lane 3; *E. coli*, lane 6) that comigrate with unmodified *B. subtilis* RNase P RNA (lane 4) or *E. coli* RNase P RNA (lane 7).

of the intermolecular cross-linked species to products migrating with radiolabeled uncross-linked RNase P RNA controls. Since the unique site of radioactive label in the cross-linking reaction was located in the single-nucleotide 5′ leader of tRNA(G-1), we conclude that the 5′ radiolabeled nucleotide was transferred to the nonradiolabeled RNase P RNA via cross-linking, followed by subsequent cleavage of the attached substrate. Experiments utilizing gel-purified cross-linked species also reacted in the presence of magnesium under dilute conditions (<0.02 nM, >160-fold below K_D) and therefore confirm that the product generated upon incubation with magnesium is derived exclusively from the original cross-linked species and that cleavage does not occur via intermolecular cleavage by unreacted ribozyme (data not shown).

DISCUSSION

Previous analyses of cleavage site recognition by the bacterial RNase P RNA using long- and short-range photoagents have detected a number of conserved elements of ribozyme structure in the vicinity of the substrate phosphate, which primarily include J5/15, J18/2, P15, and J15/16 (*16*, *17*, *19*). However, the orientation of these structural elements relative to the cleavage site is not well-defined by the current library of cross-linking and biochemical results. In this study, we have incorporated the short-range photo-cross-linking agent s^6G into the bases adjacent to the scissile phosphate of the tRNA cleavage site. Specifically, s^6G was incorporated into the 5′ end of tRNA and a substrate containing a single nucleotide leader, tRNA(G-1). Importantly, these photoaffinity probes were found to bind with similar high affinity to both *E. coli* and *B. subtilis* RNase P RNAs. In addition, the presence of s^6G in the context of the single-nucleotide leader tRNA(G-1) substrate was found to alter the rate of catalysis by the *B. subtilis* ribozyme only slightly and was found not to perturb the accuracy of cleavage. Using this experimental system, we detect a single intermolecular cross-link between the 5′ end of s^6G-modified tRNA and J5/15 in *E. coli* and *B. subtilis* RNase P RNA: A248 in *E. coli* RNase P RNA and A246 in *B. subtilis* RNase P RNA. Placing the s^6G photoagent one nucleotide upstream of the cleavage site, in tRNA(G-1), shifts the cross-linking to J18/2 with no cross-linking detected to J5/15. Like tRNA, the tRNA(G-1) probe cross-links to homologous nucleotides in both ribozymes: G332 (with minor cross-linking to A333) in *E. coli* and A318 (with minor cross-linking to U317 and G319) in *B. subtilis* RNase P RNA. These results refine our understanding of cleavage site recognition by identifing a discrete subset of residues in RNase P RNA that are in close proximity to the pre-tRNA substrate phosphate (Figure 8).

It is a formal possibility that the cross-links we detect reflect minor conformations that are in rapid equilibrium with the native structure and that cross-linking kinetically traps these minor conformational species. It is also possible that the differences in cross-linking we observe are the result of conformational differences between the complexes containing tRNA versus tRNA(G-1) substrate rather than differences in the position of the photoagent relative to the cleavage site. However, several factors indicate that these explanations are unlikely. First, the high efficiency of these cross-links at homologous positions in both classes of RNase P RNA structure argues strongly that this result represents a general feature of the ribozyme−tRNA complex. Second, in addition to the current binding studies, previous cross-linking, chemical protection, and kinetic studies (*14*, *16*, *25*, *35*) show that ribozyme complexes with tRNA and tRNAs with a single-nucleotide leader sequence are highly analogous and conformational differences between them are likely to be small. Third, cross-links between tRNA(G-1) and both ribozymes retain the ability to catalyze cleavage of the covalently attached substrate. In particular, it is important to note that unlike the considerable structural flexibility (ca. 9 Å) afforded by long-range cross-linking agents such as APA, the short-range cross-link (ca. 1.5 Å) from s^6G greatly restricts the conformational space that can be explored within the catalytically competent cross-linked complexes we observe (*44*). While it is possible for the inappropriate joining of

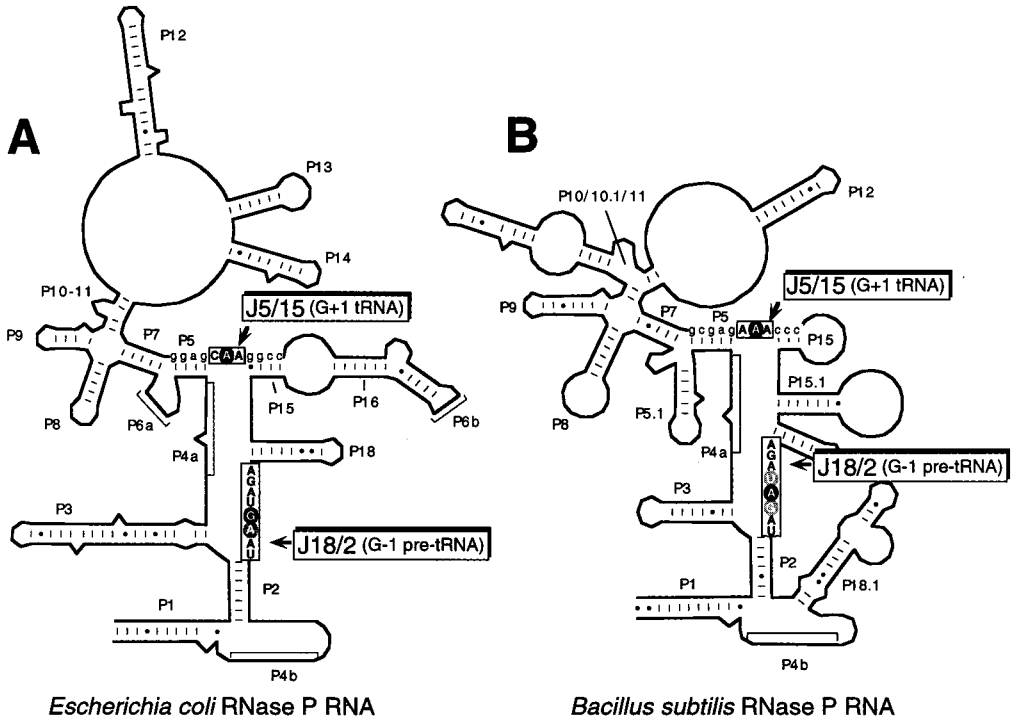

FIGURE 8: Position of intermolecular cross-links. Position of intermolecular cross-links (●) on the current two-dimensional structures of *E. coli* RNase P RNA (**A**) and *B. subtilis* RNase P RNA (**B**). Dark circles indicate main sites of cross-linking. Grey circles indicate minor sites of cross-linking. Boxes enclose secondary structure regions J5/15 or J18/2.

peripheral elements of the ribozyme−substrate complex to still allow for catalytic activity, there is likely to be little tolerance for inappropriate structural constraints in the catalytic core, particularly if the cross-link involves a conserved region of the ribozyme and the base immediately upstream of the scissile phosphate. Taken together, the data presented here strongly suggest that the observed cross-links reflect the structure of the native enzyme−substrate complex.

The short-range cross-links we observe between the 5′ end of tRNA or tRNA(G-1) and RNase P RNA also correspond well to the available cross-linking and biochemical data. In particular, while previous studies reported s^4U cross-linking from position −1 of a pre-tRNA substrate to a number of positions in *E. coli* RNase P RNA, very strong cross-linking was observed to position G332 and A333 (*19*). Importantly, the findings with s^4U were obtained with a pre-tRNA substrate containing a full-length 5′ leader, indicating that the 5′ end of tRNA(G-1) approximates the position of nucleotide −1 in a substrate with a full-length leader sequence. s^4U cross-linking from position −1 in wild-type pre-$tRNA^{Asp}$ in our laboratory also produces discrete cross-links to homologous nucleotides in *B. subtilis* RNase P RNA as observed previously in *E. coli* RNase P (Christian and Harris, unpublished results, *19*). In addition to these cross-linking experiments, chemical protection studies revealed that 5′ leader sequences of 2−4 nucleotides protect nucleotides in J18/2 at, or immediately adjacent to, the nucleotides found to cross-link to the single-nucleotide leader of tRNA(G-1) (*14*). The close proximity of position −1 in pre-tRNA to G332 (*E. coli*) in RNase P RNA, therefore, is not unique to s^6G or short-range cross-linking, but is observed by a number of experimental approaches and suggests that G332 (*E. coli*) interacts directly with the 5′ leader sequence.

Consistent with the short-range cross-linking between position +1 and A248 (*E. coli*) in J5/15 in RNase P RNA that we have observed, modification interference studies have recently demonstrated that the N7 functional group of A248 is essential for both substrate binding (Siew, Zahler, Cassano, Strobel, and Harris, unpublished results) and catalytic activity (*45*). These results suggest that position +1 may form a direct contact with the universally conserved adenosine in the center of J5/15, and thus may provide an important element in cleavage site recognition. Indeed, the current work and the available biochemical data suggest that both J18/2 and J5/15 are likely to perform important roles in positioning the pre-tRNA cleavage site within the active site.

The close proximity of position +1 and J5/15 also provides an important refinement in low-resolution models of the ribozyme−tRNA complex. Chemical cross-linking, mutagenesis, and phylogenetic comparative studies have yielded a collection of constraints for development of two very similar low-resolution three-dimensional models for the *E. coli* and *B. subtilis* ribozymes (*18*, *46*). The positions and orientation of individual helices are generally well-defined (ca. 5−10 Å) and in some cases regions of RNase P RNA are well-constrained relative to tRNA. Positions in RNase P RNA adjacent to the cleavage site, however, are poorly constrained in these models; the only distance constraint is to position +1 from long-range cross-linking studies with APA (*16*). The short-range cross-linking of the 5′ end of tRNA to J5/15 (this study) and the interaction of the 3′ CCA sequence of tRNA with J16/15 (*13*) puts the base of the acceptor stem in close proximity to helix P15. However, both three-dimensional models (*18*, *44*) place the interaction between the 3′ CCA and J15/16 in the minor groove side of P15, making it difficult to satisfy the structural constraint between the 5′ end of tRNA and J5/15 without significant rearrangement of the model structures. Nucleotide position +1 at the tRNA cleavage site and A248 in J5/15 of *E. coli* RNase P are positioned approximately 15 Å apart in the

recent model of the ribozyme−substrate complex by Pace and co-workers (*18*), while the corresponding cross-linked nucleotides are positioned approximately 24 Å apart in the model from Massier et al. (*46*). Position −1 is only modeled in the three-dimensional structure by Massier et al. (*46*) but again is positioned approximately 10 Å from G332 in J18/2, further than the distance implied by the available cross-linking and chemical protection results. Both of these models, therefore, require significant refinement to accommodate the present data as positional constraints. The current cross-linking data may be satisfied by placing the 3′ CCA interaction on the major-groove side of P15 and rearranging the modeled structure of the P15−P16 internal bulge, though, as yet, there is insufficient structural information to model this region in detail. The strong correspondence between the current cross-linking study and the available biochemical data suggests that the results reported here can be used in refining low-resolution models and targeting residues for mutagenic analysis. Detailed structural modeling and understanding of the three-dimensional environment around the cleavage site must, however, await the identification of specific interactions such as those implied by the current study. The identification of these interactions is likely to elucidate the mechanism by which the pre-tRNA substrate is oriented in the ribozyme's active site and possibly identify elements of the active site itself.

ACKNOWLEDGMENT

We gratefully acknowledge Dr. Vernon Anderson for the NMR analysis of the s^6GMP and thank Dr. Timothy Nilsen, Dr. Jonatha Gott, Nicholas Kaye, Frank Campbell, Adam Cassano, and Nathan Zahler for discussion and careful reading of the manuscript.

REFERENCES

1. Altman, S., Kirsebom, L. A., and Talbot, S. (1995) in *tRNA, Structure, Biosynthesis and Function* (Soll, D., and RajBhandary, U., Eds.) pp 67−78, American Society for Microbiology Press, Washington, DC.
2. Harris, M. E., Frank, D. N., and Pace, N. R. (1998) in *RNA Structure and Function*, pp 309−337. Cold Spring Harbor Laboratory Press, Plainview, NY.
3. Haas, E. S., and Brown, J. W. (1998) *Nucleic Acids Res.* (in press).
4. Guerrier-Takada, C., Gardiner, K., Marsh, T., Pace, N., and Altman, S. (1983) *Cell 35*, 849−857.
5. Kruz, J., Niranjanakumari, S., and Fierke, C. A. (1998) *Biochemistry 37*, 2393−2400.
6. Crary, S. M., Niranjanakumari, S., and Fierke, C. A. (1998) *Biochemistry 37*, 9409−9416.
7. James, B. D., Olsen, G. J., Liu, J., and Pace, N. R. (1988) *Cell 52*, 19−26.
8. Haas, E. S., Brown, J. W., Pitulle, C., and Pace, N. R. (1994) *Proc. Natl. Acad. Sci. U.S.A. 91*, 2527−2531.
9. Brown, J. W. (1997) in *The RNase P Database*, http://jwbrown.mbio.ncsu.edu/RNaseP/home.html.
10. Nolan, J. M., Burke, D. H., and Pace, N. R. (1983) *Science 261*, 762−765.
11. Pan, T., Loria, A., and Zhong, K. (1995) *Proc. Natl. Acad. Sci. U.S.A. 95*, 12510−12514.
12. Loria, A., and Pan, T. (1997) *Biochemistry 36*, 6317−6325.
13. Kirsebom, L. A., and Svärd, S. G. (1994) *EMBO J. 13*, 4870−4876.
14. LaGrandeur, T. E., Hüttenhofer, A., Noller, H. F., and Pace, N. R. (1994) *EMBO J. 13*, 3945−3952.
15. Oh, B.-K., and Pace, N. R. (1994) *Nucleic Acids Res. 22*, 4087−4094.
16. Burgin, A. B., and Pace, N. R. (1990) *EMBO J. 9*, 4111−4118.
17. Harris, M. E., Nolan, J. M., Malhorta, A., Brown, J. W., Harvey, S. C., and Pace, N. R. (1994) *EMBO J. 13*, 3953−3963.
18. Chen, J.-L., Nolan, J. M., Harris, M. E., and Pace, N. R. (1998) *EMBO J. 17*, 1515−1525.
19. Kufel, J., and Kirsebom, L. A. (1996) *Proc. Natl. Acad. Sci. U.S.A. 93*, 6085−6090.
20. Svärd, S. G., and Kirsebom, L. A. (1993) *Nucleic Acids Res. 21*, 427−434.
21. Kufel, J., and Kirsebom, L. A. (1994) *J. Mol. Biol. 244*, 511−521.
22. Kunst, F., Ogasawara, N., Moszer, I., et al. (1977) *Nature 390*, 249−256.
23. Blattner, F. R., Plunkett, G., Bloch, C. A., et al. (1997) *Science 277*, 1453−1474.
24. Svärd, S. G., and Kirsebom, L. A. (1992) *J. Biol. Chem. 267*, 2429−2436.
25. Smith, D., and Pace, N. R. (1993) *Biochemistry 32*, 5273−5281.
26. Tallsjo, A., and Kirsebom, L. A. (1993) *Nucleic Acids Res. 21*, 51−57.
27. Loria, A., and Pan, T. (1998) *Biochemistry 37*, 10126−10133.
28. Kahle, D., Kust, B., and Krupp, G. (1993) *Biochimie 75*, 955−962.
29. Warnecke, J. M., Furste, J. P., Hardt, W., Erdmann, V. A., and Hartmann, R. K. (1996) *Proc. Natl. Acad. Sci. U.S.A. 93*, 8924−8928.
30. Chen, Y., Li, X., and Gegenheimer, P. (1997) *Biochemistry 36*, 2425−2438.
31. Sergiev, P. V., Lavrik, I. N., Wlasoff, V. A., Dokudovskaya, S. S., Dontsova, O. A., Bogdanov, A. A., and Brimacombe, R. (1997) *RNA 3*, 464−475.
32. Beebe, J. A., and Fierke, C. A. (1994) *Biochemistry 33*, 10294−10304.
33. Silberklang, M., Gillum, A. M., and RajBhandary, U. L. (1979) *Methods Enzymol. 59*, 58−109.
34. Esteban, J. A., Banerjee, A. R., and Burke, J. M. (1997) *J. Biol. Chem. 272*, 13629−13639.
35. Reich, C., Olsen, G. J., Pace, B., and Pace, N. R. (1988) *Science 239*, 178−181.
36. Penefsky, H. S. (1979) *Methods Enzymol. 56*, 527−530.
37. Sambrook, J., Fritsch, E. F., and Maniatis, T. (1989) *Molecular Cloning: A Laboratory Manual*, 2nd ed., pp 6.36 and E.37, Cold Spring Harbor Laboratory Press, Plainview, NY.
38. Burkard, U., Willis, I., and Söll, D. (1988) *J. Biol. Chem. 263*, 2447−2451.
39. Green, C. J., and Vold, B. S. (1988) *J. Biol. Chem. 263*, 652−657.
40. Kirsebom, L. A., and Svärd, S. G. (1992) *Nucleic Acids Res. 20*, 425−432.
41. Smith, D., Burgin, A. B., Haas, E. S., and Pace, N. R. (1992) *J. Biol. Chem. 267*, 2429−2436.
42. Harris, M. E., Kazantsev, A., Chen, J.-L., and Pace, N. R. (1997) *RNA 3*, 561−576.
43. Ehresmann, C., Baudin, F., Mougel, M., Romby, P., Ebel. J.-P., Ehresmann, B (1987) *Nucleic Acids Res. 15*, 9109−9128.
44. Favre, A., Saintome, C., Fourrey, J. L., Clivio, P., and Laugaa, P. (1998) *J. Photochem. Photobiol. 42*, 109−124.
45. Kazantsev, A. V., and Pace, N. R. (1998) *RNA 4*, 937−947.
46. Massier, C., Jaeger, L., and Westhof, E. (1998) *J. Mol. Biol. 279*, 773−793.

BI982050A